Received: 14 May 2025 | Revised: 17 July 2025 | Accepted: 9 September 2025 | Published online: 30 September 2025

RESEARCH ARTICLE

Archives of Advanced Engineering Science
2025, Vol. 00(00) 1–14
DOI: 10.47852/bonviewAAES52026150

BON VIEW PUBLISHING

Numerical Study on Toppling Mechanisms of Crane and Pile Driver Based on Structural Stability Theory

Shouji Toma[1,*] and Wai Fah Chen[2]

[1] *Hokkai-Gakuen University and Taiki Consultant Co. Ltd., Japan*

[2] *University of Hawaii, USA*

Abstract: This paper presents a numerical investigation into the theoretical safety criteria for the toppling of cranes and pile drivers by providing sample calculations and expanding on previously published theoretical work, in which the fundamental elements, such as the structural model, the classification of toppling modes, etc., are developed. It is believed that the frequent occurrences of crane and pile driver toppling are closely related to structural instability within their toppling mechanisms. The conventional evaluation method for toppling stability, which is based on the overturning moment approach, may not sufficiently address the mechanisms of toppling on soft ground. In fact, many toppling accidents show signs of inadequate ground strength, such as ground failure. This issue likely involves not only a lack of ground strength to withstand the bearing pressure from crawlers or outriggers but also insufficient deformation performance (stiffness) of the ground. In structural stability theory, an important factor in assessing the required ground stiffness is the height of the applied load. Conventional toppling stability assessments assume that if the overturning moment is the same, the stability will also be the same. However, from the perspective of structural stability theory, toppling can occur even when the overturning moment is zero in extreme cases with weak ground stiffness and large load height. This study aims to look for the influence on the toppling mechanism by presenting sample calculations for a simple analytical model under various operational conditions—including load height, ground stiffness, and working radius—to better define the criteria for toppling.

Keywords: toppling mechanism, crane toppling, pile drivers, structural stability, soft foundation, toppling safety, toppling criteria

1. Introduction

This paper is a numerical investigation to verify the theoretical safety criteria for toppling of crane and pile driver, which was published previously [1]. Topple-over accidents involving heavy machinery such as cranes, pile drivers, aerial work platforms, jacks, etc., have occurred repeatedly [2, 3]. These topple-over incidents share many common characteristics; however, in this study, the crawler crane with high centers of gravity, as illustrated in Figure 1, is focused.

There were a number of researches on this toppling issue from different points of view including crane operations [4], boom luffing motion [5], zero moment point theory [6], electrical resistivity measurement system [7], the Queensland Code of Practice [8], overturning moment caused by sway [9], geotechnical engineering [10], consideration of possible ground failure [11], etc. Furthermore, in Japan, Tamate et al. investigated the safety requirements for preventing the toppling of pile drivers [12, 13].

This paper aims to clarify whether structural instability problems are associated with these incidents. Topple-over issues can be classified into two types: the "overturning moment type" and the "structural instability type" [14]. Traditionally, stability design for cranes and similar equipment has been based on the overturning moment type. However, this study focuses on the structural instability type, which is a different approach from the conventional stability assessment.

Figure 1
Crawler crane and pile driver

***Corresponding author:** Shouji Toma, Hokkai-Gakuen University, Japan. Email: toma@hgu.jp

A commonly experienced phenomenon is the increased instability when standing on a boat. This is likely due not only to an increase in overturning moment but also to an increase in instability caused by the higher point of load application. Similar to the toppling of heavy machinery, structural instability theory can also be applied to capsizing problems in floating bodies with high centers of gravity, and correlations have been noted with traditional maritime stability evaluation methods [15]. In particular, the floating stability of a rectangular vessel with a high center of gravity, such as the Self-Elevating Platform, was investigated by applying the structural stability approach [16, 17].

Compared to a classic example of a structural instability problem, elastic buckling of a long column, the height of the center of gravity in toppling problems corresponds to the member length, and the stiffness of the supporting ground corresponds to the flexural stiffness of the column member. Just as a long column can bend even with zero bending moment, heavy machinery can topple over even when the overturning moment is zero. Furthermore, previous studies have shown that, in addition to static analysis, dynamic analysis reveals that the presence of inertial forces makes toppling even more likely [14].

In topple-over problems involving top-heavy machinery, three key factors are considered to be deeply interconnected: overturning moment, ground strength, and the height of the center of gravity. Among these, the conventional overturning moment approach evaluates stability based on two factors—overturning moment (a function of load and working radius) and ground strength. In contrast, the structural instability approach incorporates an additional factor: the height of the center of gravity (load height). According to the structural instability model, even when the overturning moment and ground strength are the same, a greater load height makes toppling more likely. Furthermore, the presence of dynamic inertial forces, such as those generated during rotating boom motion and while in transit, further increases the risk of toppling.

This paper focuses to investigate theoretically the influence of the height of the load (center of gravity), a crucial factor in the cause of toppling accidents, and presents specific numerical calculation examples to clarify its impact. In order to achieve this, the paper adopts an elastic-static analysis for simplicity in the structural model and analytical procedures. Nevertheless, it is believed that the paper will demonstrate how the instability is involved in the toppling mechanisms of heavy machinery.

2. Evaluation of Toppling Stability

2.1. Overview of structural instability

In this study, cranes and pile drivers placed on soft ground are modeled as a simplified structural system comprising a rigid bar and a rotational spring, as illustrated in Figure 2 [14]. Therefore, a crane does not deform but rotates only at the supporting point, which expresses the entire stiffness of the ground foundation. For further simplification, eccentric loading is not considered. Even with the simplest model shown in Figure 2, it is believed that numerical analysis can describe the effect of structural stability on toppling mechanisms.

This structural system in Figure 2 has an elastic critical load, expressed by the following equation [14]:

$$P_{cr} = K_S / L \tag{1}$$

where P_{cr} = elastic critical load, K_S = rotational spring stiffness of the supporting ground, L = load height (member length).

Equation (1) corresponds to the elastic buckling load for a long column (Euler load). Both critical loads, P_{cr} in Equation (1) and

Figure 2
Rigid bar-rotational spring model

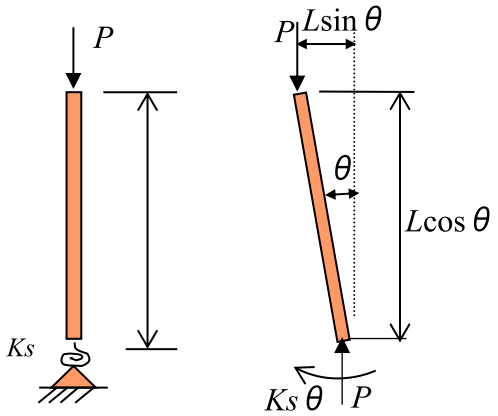

Figure 3
Stability surface

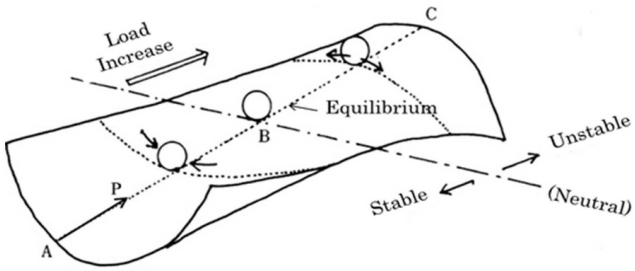

Euler load, are well-known elastic limits in structural engineering. When the applied load exceeds this critical value, the crane or pile driver becomes unstable and topples over. What is noteworthy is that the rigid bar satisfying Equation (1) is in an upright position: thus, the overturning moment is zero. The usefulness of the critical load expression in Equation (1), which forms the foundation of structural stability theory, has been validated through finite element analysis [14] and experiments using floating bodies [15]. For further details on these structural instability problems, the reader is referred to previous literature [1, 14, 15]. In the context of the structural stability theory discussed here, the ground is assumed to behave as an elastic body. The overall stiffness (deformation performance) of the ground is represented by a linear rotational spring stiffness K_S as seen in Equation (1) and Figure 2.

The boundary between stable and unstable conditions (the critical load) is illustrated as the neutral point of a concave-convex surface in Figure 3. A stable state is represented by a ball on a concave surface in Figure 3 or by Figure 4(a), where a displaced ball returns to its original position. Conversely, an unstable state is depicted as a ball on a convex surface in Figure 3 or in Figure 4(c), where a displaced ball inevitably falls. In other words, in an unstable state, deformation is not reversible.

A distinctive characteristic of the structural instability type is that, much like a ball rolling off a slope in the unstable region shown in Figure 3, once displacement begins, it is difficult to arrest, and the structure often proceeds rapidly to complete toppling. In the cases where toppling occurs due to the overturning moment, the neutral point is represented by the condition in Figure 4(b), where the load and the reaction force are aligned vertically. The angle at this state is defined as the *stability limit angle (or toppling angle)* [1, 14]. At the same time, in the structural stability model (buckling-type of toppling), the critical load given by Equation (1) also represents a neutral condition. Thus, toppling can occur even with zero overturning

Figure 4
Concept of Stable and Unstable

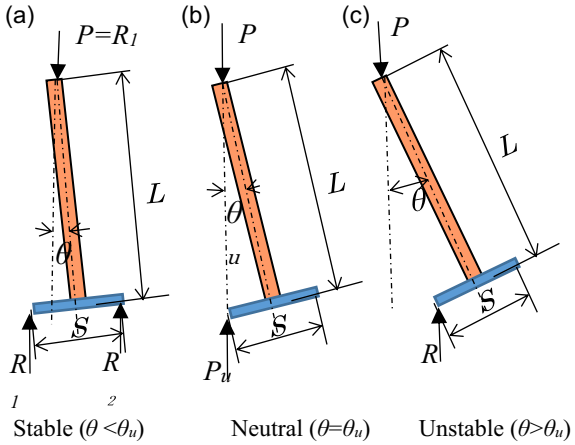

Figure 5
Critical load-height curves

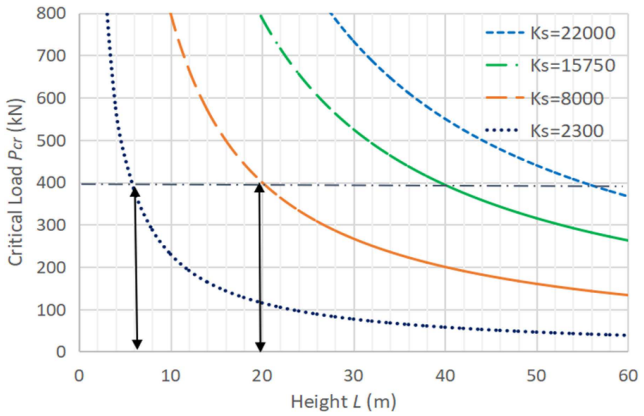

moment if this critical load is exceeded. In toppling problems, these two neutral conditions are interrelated.

In the overturning moment type, stability is evaluated by comparing the maximum ground contact pressure with the ground's bearing strength. In contrast, in the structural stability type, stability depends on the deformation performance of the ground, represented by the rotational spring stiffness K_S in Equation (1). Assuming this rotational spring stiffness is constant, Equation (1) shows that the relationship between the critical load and its height of application is inversely proportional, as illustrated in Figure 5 [14]. For example, as shown in the figure, if the applied load is fixed at 400 kN, toppling occurs at a load height of 20 m when the ground's rotational stiffness is K_S = 8000 kNm/rad., while toppling occurs at a lower height of 6 m when the stiffness is weaker at K_S = 2300 kNm/rad. Furthermore, if the ground stiffness K_S is held constant, there exists a range where the critical load P_{cr} rapidly decreases as the load height increases.

This clearly indicates the significant influence of load height on toppling problems. Moreover, this influence applies not only to the ideal upright condition (where the overturning moment is zero), as described in Equation (1), but also to more general operating conditions involving initial inclinations (i.e., when an overturning moment is present), which will be discussed later in Equation (3).

Figure 6
Working radius and boom length (SCX400)

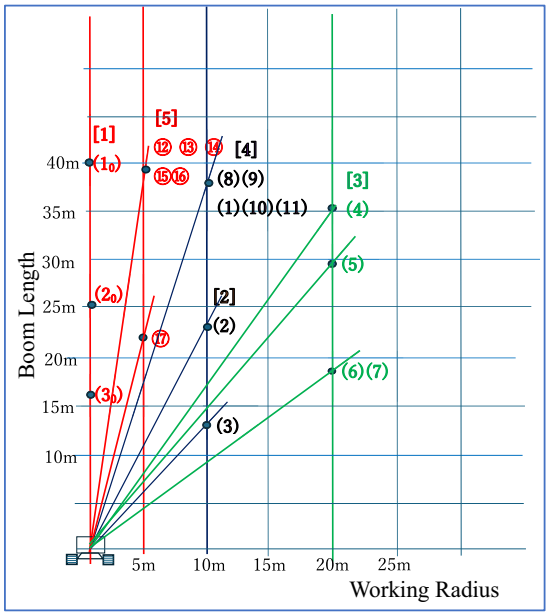

Table 1
Rated total load (SCX400)

unit: tonf

Operating Radius (m)	Boom Length (m) 16	22	25	34	40
4.0	4.2/32.65				
4.5	29.30				
5.0	25.00	5.3/22.85	⑰		
5.5	21.75	21.65	5.8/20		
6.0	19.20	19.10	19.05		
7.0	15.55	15.45	15.35	7.5/13.75	
8.0	13.00	12.90	12.80	12.60	8.6/10.4
9.0	11.10	11.00	10.95	10.70	10.25
10.0	(3) 9.7	9.55	(2) 9.5	9.25	(1) 9.15 (8)(9)(10)(11)
12.0	7.65	7.55	7.45	7.20	7.10
14.0	6.30	6.15	6.05	5.80	5.70
16.0	14.9/5.8	5.15	5.05	4.80	4.70
18.0		4.40	4.30	4.05	3.90
20.0		3.80	(6)(7) 3.7	(5) 3.45	(4) 3.3

Note: This table is excerpted from "HITACHI SUMITOMO SCX400 HYDRAULIC CRAWLER CRANE Specifications" [20].

2.2. Current stability evaluation

The current stability evaluation criteria for cranes and similar equipment are fundamentally based on the *working range diagram* (boom length vs. operating radius relationship) shown in Figure 6 and the *rated total load table* in Table 1 [18]. The numbered calculation conditions used in later examples are indicated in these diagrams and tables (for details, see Tables 2 and 3). The current stability evaluation is based on the principle that the overturning moment caused by the loads must not exceed the resisting moment provided by the ground. A fundamental assumption in this evaluation is that the ground strength must be sufficient to withstand the maximum contact pressure induced by the overturning moment.

Table 2
Calculated results ([1–4])

Row No.	Item	[1] $\theta_0 = 0$, P_u = 10 t			[2] P_u = 10 t, a = 10 m			[3] $P_u \fallingdotseq 5$ t, a = 20 m				[4] L_B = 40 m, a = 10 m				Item
		(1_0)	(2_0)	(3_0)	(1)	(2)	(3)	(4)	(5)	(6)	(7)	(8)	(9)	(10) = (1)	(11)	
(a)	P_u (tonf)	10	10	10	10	10	10	4.65	4.84	5.1	5	5	7.5	10	12.5	P_u (tonf)
(b)	L_B (m)	40	25	16	40	25	16	40	34	25	25	40	40	40	40	L_B (m)
(c)	a (m)	0	0	0	10	10	10	20	20	20	20	10	10	10	10	a (m)
(d)	θ_0 (deg.)	0	0	0	12.3	20	32.4	27.6	33.1	48.1	48.1	12.3	12.3	12.3	12.3	θ_0 (deg.)
(e)	θ_0 (rad.)	0	0	0	0.215	0.349	0.565	0.482	0.578	0.840	0.840	0.215	0.215	0.215	0.215	θ_0 (rad.)
(f)	Wt (tonf)	54.2	53.1	52.5	54.2	53.1	52.5	49.1	48.9	48.2	48.1	49.2	51.7	54.2	56.7	Wt (tonf)
(g)	R_A (tonf)	27.1	26.55	26.25	47.8	45.5	44.3	49	48.8	48.1	47.5	30.1	39	47.8	56.6	R_A (tonf)
(h)	R_B (tonf)	27.1	26.55	26.25	6.4	7.6	8.2	0.1	0.1	0.1	0.6	19.1	12.8	6.4	0.1	R_B (tonf)
(i)	max p (kgf/cm^2)	≒0.82	≒0.80	≒0.799	3.32	2.98	2.82	5.69	5.69	5.43	5.01	1.3	2.09	3.32	6.24	max p (kgf/cm^2)
(j)	Mt (tonf·m)	0	0	0	68.3	67.5	59.6	80.7	80.3	79.2	77.4	17.8	43.4	68.3	93.2	Mt (tonf·m)
(k)	Current Standards Rated Total Load: P_{rat} (tonf)	-	-	-	9.15	9.5	9.7	3.3	3.45	3.7	3.7		9.15			Current Standards Rated Total Load: P_{rat}
(l)	g (m)	1.65	1.65	1.65	2.910	2.828	2.785	3.293	3.293	3.293	3.259	2.019	2.489	2.910	3.294	g (m)
(m)	e (m)	0	0	0	1.260	1.178	1.135	1.643	1.643	1.643	1.609	0.369	0.839	1.260	1.644	e (m)
(n)	L = e/sinθ_0 (m)	40	25	16	5.916	3.443	2.117	3.547	3.009	2.208	2.162	1.732	3.940	5.916	7.718	L = e/sinθ_0 (m)
(o)	θ_u (rad.)	0.041	0.066	0.103	0.283	0.4997	0.893	0.484	0.580	0.844	0.868	1.262	0.432	0.283	0.215	θ_u (rad.)
(p)	θ_0 / θ_u	0	0	0	0.760	0.699	0.633	0.996	0.995	0.994	0.967	0.170	0.497	0.760	0.996	θ_0 / θ_u
(q)	$P_u/P_{cr} = 1–\theta_0 / \theta_u$	1	1	1	0.240	0.301	0.367	0.0044	0.0046	0.0055	0.0334	0.830	0.503	0.240	0.004	$P_u/P_{cr} = 1-\theta_0 / \theta_u$
(r)	P_{cr} (tonf)	10	10	10	41.6	33.2	27.2	1051.7	1048.3	924.7	149.8	6.0	14.9	41.6	3489.0	P_{cr} (tonf)
(s)	$K_s = P_{cr}$ L(tonf·m/rad.)	400	250	160	246	114	58	3730	3155	2041	324	10	59	246	26929	$K_s = P_{cr}$ L(tonf·m/rad.)
(t)	kv (tonf/cm)	0.73	0.46	0.29	0.45	0.21	0.11	6.85	5.79	3.75	0.59	0.02	0.11	0.45	49.46	kv (tonf/cm)
(u)	d (cm)	36.9	57.8	89.3	105.8	216.9	418.2	7.2	8.4	12.8	79.9	1571.0	361.6	105.8	1.1	d (cm)

Notes: (1) The rows (a)~(e) are calculation conditions, and (f)~(k) are based on the “Crane Ground Pressure Simulation (SCX400)” by Sumitomo Heavy Industries Construction Crane Co., Ltd.
(2) The rows (p)~(u) indicate the values at the time of of toppling.
(3) The maximum ground pressure (max p) is for the slewing direction where the value is at its highest, and the distribution shape is trapezoidal or triangular.
(4) Condition [1] is just for reference; P cr and L are assumed to be the load P u and the member length L B, respectively, which diffes from other cases.
(5) Acording to “SCX400 Hydraulic Crawler Crane Specifications”, the above rated total load Prat is 78% of the toppling load.

Table 3
Calculated results ([5])

	[5] L_B = 40 m, θ_0 = 5 deg.					L_B = 22m
Item	⑫	⑬	⑭	⑮	⑯	⑰
P_u (tonf)	15	20	25	30	35	35
L_B (m)	40	40	40	40	40	22
a (m)	5	5	5	5	5	5
θ_0 (deg.)	5	5	5	5	5	13
θ_0 (rad.)	0.0873	0.0873	0.0873	0.0873	0.0873	0.2269
Wt (tonf)	59.3	64.3	69.3	74.3	79	77.9
R_A (tonf)	39.5	49.5	59.5	69.5	79	60.5
R_B (tonf)	19.8	14.8	9.8	4.8	0	17.4
max p (kgf/cm^2)	1.85	2.71	3.87	5.66	8.83	3.33
Mt (tonf·m)	32.5	57.2	82	106.8	130.3	71.1
Current Standards Rated Total Load: P_{rat} (tonf)			Out of range			5.3/ 22.85
g (m)	2.198	2.540	2.833	3.087	3.300	2.563
e (m)	0.548	0.890	1.183	1.437	1.650	0.913
L = e/sinθ_0 (m)	6.289	10.217	13.577	16.486	18.932	4.058
θ_u (rad.)	0.265	0.162	0.122	0.100	0.087	0.419
θ_0 /θ_u	0.329	0.538	0.716	0.870	1.000	0.542
P_u/P_{cr} = 1-θ_0 /θ_u	0.671	0.462	0.284	0.130	0.000	0.458
P_{cr} (tonf)	22.3	43.3	88.1	231.6	∞	76.4
$K_s = P_{cr}$ L(tonf·m/rad.)	141	442	1196	3817	∞	310
kv (tonf/cm)	0.26	0.81	2.20	7.01	∞	0.57
d (cm)	153.0	60.9	27.1	9.9	0.0	106.2

In the preparation of the working range diagram (Figure 6) and the rated total load table (Table 1), the ground is assumed to be level and firm. Therefore, ground deformation is not taken into account. If the ground is weak and susceptible to deformation, ground improvement measures such as soil stabilization or steel plates are required.

When a toppling accident occurs, investigations into the cause focus on comparing the maximum acting contact pressure with the ground strength. This method of stability evaluation corresponds to the overturning moment type among the toppling causes classified within the framework of structural stability theory [1]. In the overturning moment type, stability is evaluated based on whether the overturning moment exceeds the resisting moment, as expressed in the following equation:

$$M_t > M_r \tag{2}$$

in which M_t = overturning moment, M_r = resisting moment.

The judgment of toppling is not limited to the comparison of moments in Equation (2); as mentioned earlier, it is also assessed by comparing the maximum contact pressure of the crawler with the bearing capacity of the ground. According to the current evaluation method, if the load and working radius are the same, the overturning moment will also be the same regardless of the load height (when ignoring differences in boom weight), and thus, the maximum contact pressure will be the same.

Moreover, under this method, toppling is assumed not to occur unless a toppling moment acts on the system. However, as explained in the previous section, structural stability theory suggests that toppling may occur depending on the height of the load—even in the absence of an overturning moment—highlighting a major difference between the two approaches.

The rotational spring stiffness (or settlement) used in structural stability theory is also referenced in the *Maintaining Support Foundation for Mobile Crane, Pile Driver, etc.* [19], where it is used as a criterion for determining the necessity of steel plates or ground improvement in Japan. However, in the current toppling stability evaluation method (the overturning moment type), there may be a problem in assuming that the ground becomes sufficiently firm simply through surface preparation. When the load height is large, insufficiently stiff ground—even after preparation—can still lead to toppling. The structural stability theory discussed here aims to clarify the necessary ground stiffness in such cases.

2.3. Evaluation based on structural stability theory

As mentioned above, the current method of toppling stability evaluation, known as the "overturning moment type," assesses stability based on the ground bearing capacity against the maximum ground pressure applied at a certain point, without considering the deformation performance of the ground. In contrast, the structural stability type expresses the stiffness (deformation performance) of

Figure 7
Load-displacement curves

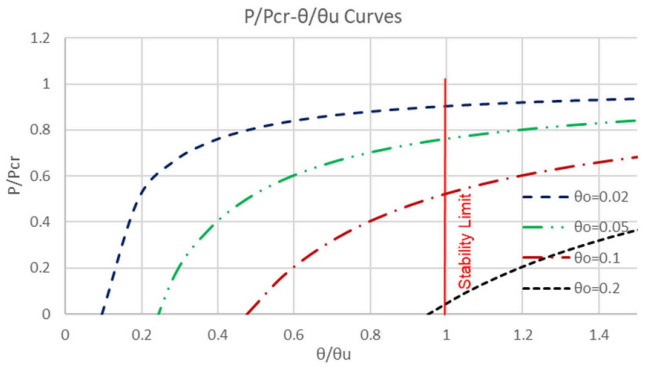

the supporting ground with rotational spring stiffness, which is used in the stability evaluation.

The structural model of the pile driver or crane is represented by a rigid bar–rotational spring system as shown in Figure 2, and its critical load (toppling load) is given by Equation (1). From this equation, it can be seen that not only the magnitude of the load but also its height (boom length) is an important factor. In fact, toppling accidents involving cranes, pile drivers, jacks, or aerial work platforms are generally believed to occur when the point of load application is high. This suggests the importance of the height at which the load acts.

Using the structural model shown in Figure 2, the load–deformation curve can be derived, as illustrated in Figure 7 [14]. In this figure, the vertical axis represents the toppling load nondimensionalized by the critical load P_{cr}, which is defined by Equation (1), while the horizontal axis represents the deformation angle nondimensionalized using the stability limit angle (toppling angle) θ_u shown in Figure 4(b). The value of θ_u on the horizontal axis corresponds to the neutral value of the stability limit angle, and the corresponding vertical value represents the neutral value of the toppling load (refer to the stability surface in Figure 3). Thus, the intersection of the load and the stability limit angle in Figure 7 represents the toppling load P_u. From this fact, the following Equation (3) can be derived [1]:

$$\frac{P_u}{P_{cr}} + \frac{\theta_0}{\theta_u} = 1 \tag{3}$$

in which P_u = ultimate load (toppling load), P_{cr} = elastic critical load (see Eq. (1)), θ_0 = initial inclination angle and θ_u = toppling angle.

It should be noted that this formulation assumes the small-angle approximation, that is, $\sin\theta \approx \theta$. In Equation (3), the first term represents the limit value associated with the buckling-toppling mode defined by structural stability theory, while the second term corresponds to the limit value based on the current overturning moment approach.

Equation (3) represents a linear inverse relationship between the buckling-toppling mode (first term) and the overturning moment toppling mode (second term), indicating the relative contributions of each to the stability limit. The load term (first term) on the vertical axis reflects the characteristics of the ground, increasing as the ground becomes softer, while the inclination term (second term) on the horizontal axis increases as the overturning moment approaches the resisting moment. Using Equation (3), the load-displacement relationships can be illustrated in Figure 8.

Figure 8
Toppling safety (static analysis)

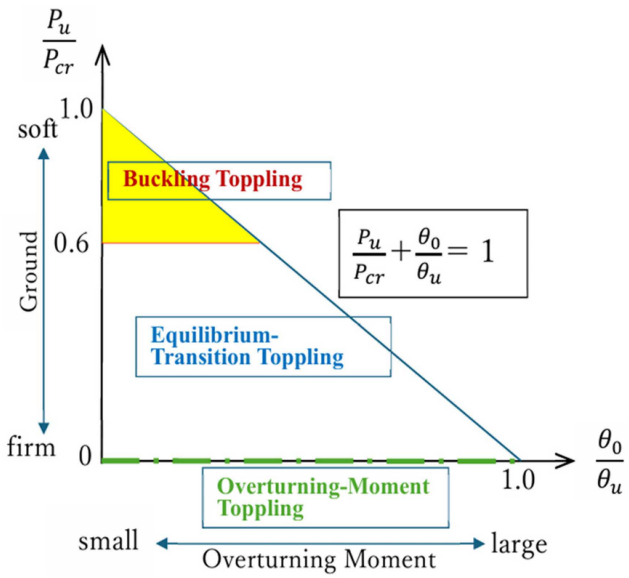

A state inside the diagonal line of Figure 8 indicates stability against toppling, while a state outside this region implies instability. Thus, Equation (3) defines the boundary between stability and instability, and each term corresponds to the neutral values on the stability surface shown in Figure 3.

In this context, the load term on the vertical axis is closely associated with load height through the critical load P_{cr}, as defined in Equation (1). As illustrated in Figure 8, toppling behavior can be categorized as follows: when the load on the vertical axis is large and dominates the toppling mechanism, the system exhibits a "*buckling-toppling*"; when the load is small and the ground is sufficiently firm such that the overturning moment dominates, the system follows an "*overturning moment toppling*." The intermediate region between these two extremes is classified as the "*equilibrium-transition toppling*" [1].

From Equation (3) and Figure 7, it is evident that the load–deformation curve is significantly influenced by the initial inclination angle θ_0. In particular, when the load ratio P/P_{cr} exceeds 0.6, deformation increases rapidly. This is not only due to an increase in the applied load P but also because the critical load P_{cr} decreases as the load height L increases (see Equation (1)), thereby increasing the value of P/P_{cr}, which leads to a higher risk of toppling. In construction site environments, such as those where cranes or pile drivers are operated, the ground conditions can rarely be considered perfectly firm, and there exist significant uncertainties with respect to the ground stiffness K_S. Therefore, to ensure safety, it is desirable to maintain $P/P_{cr} < 0.6$ [1]. This is shown by the colored triangle in Figure 8.

Conventional toppling stability assessment (as presented in Table 1, rated total load) determines the operational limit of the suspended load based on the boom length and operating radius diagram (Figure 6), along with the magnitude of the overturning moment. Stability is then evaluated by comparing this overturning moment with the resisting moment derived from the ground strength. As previously mentioned, this method belongs to the "overturning moment type" category [1]. Since the overturning moment type assumes a horizontally rigid ground, it effectively treats the critical load P_{cr} as infinite. Consequently, in the stability characteristic diagram shown in Figure 8, the term P_u/P_{cr} becomes zero, meaning that stability

is evaluated along the horizontal axis. However, in real-world field conditions, it is unrealistic to assume $P_{cr} = \infty$; rather, the ground inevitably possesses some degree of softness. It is considered that the influence of the vertical axis component in Figure 8, representing structural stability theory, underlies many unexpected toppling accidents.

The load–deformation angle curves shown in Figure 9 represent an equilibrium condition under the assumption that the load increases statically over a sufficient period. When the load is applied at a certain rate, the system is expected to follow a sloped path, such as the trajectory A → B′ shown in Figure 9(a), rather than remaining on the equilibrium curve [14]. At this point, the deformed state B′ deviates from the equilibrium path and becomes unbalanced, prompting a transition toward a new equilibrium point C. In static analysis, the system is assumed to stop at point C.

In contrast, under dynamic analysis, inertia forces come into play, as illustrated in Figure 9(b), causing the deformation to extend beyond point C to point D′. If, at this stage, the deformation exceeds the stability limit angle, toppling occurs. This type of failure is referred to as the "equilibrium-transition toppling."

The stability criterion represented in Figure 8 is based on static analysis. When the influence of inertia forces in dynamic analysis is considered, the actual stability range becomes considerably narrower, as depicted in Figure 10 [1]. Figure 10 also illustrates a safety zone that accounts for dynamic analysis and additional safety margins and is proposed as a design guideline in planning and engineering practice.

Figure 9
Comparisons between static and dynamic analyses

(a) **Static analysis**

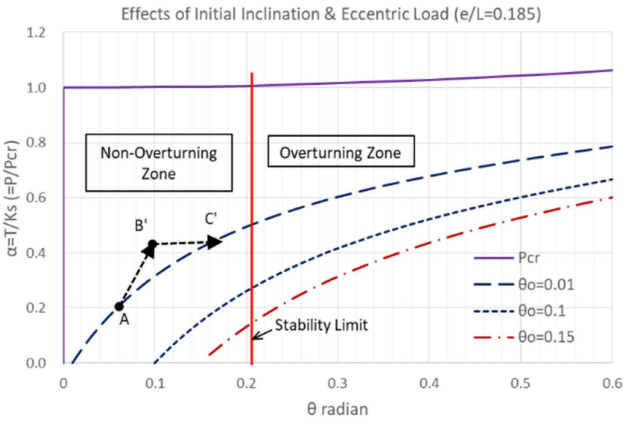

(b) **Dynamic analysis**

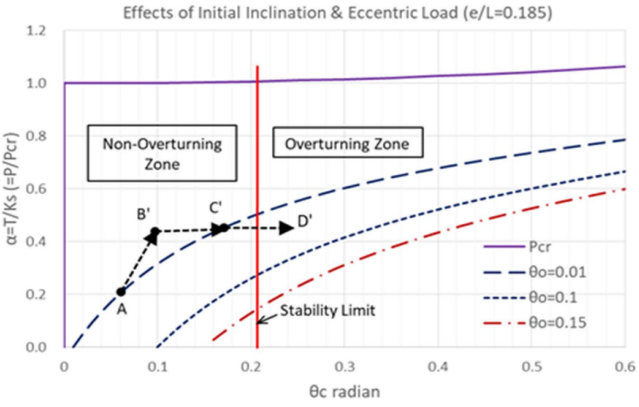

Figure 10
Toppling safety (dynamic analysis)

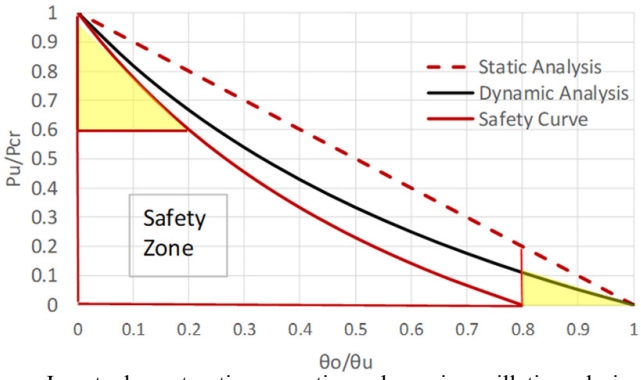

In actual construction operations, dynamic oscillations during movement or operation are considered unavoidable, and their influence is presumed to be significant. However, for the sake of clarity and ease of understanding, a simplified static analysis is adopted in this study. In static analysis, it is permissible to consider the center of gravity that integrates the distribution of dispersed mass. In contrast, dynamic analysis must account for the distribution of individual masses as inertia forces involving the second moments become relevant [14].

As discussed above, toppling of cranes and similar equipment should not be assessed solely based on local contact pressures. A more rational approach involves evaluating the overall deformation performance (rotational spring stiffness) of the crawler's ground contact area, using Equations (1) and (3).

3. Calculation Example Based on Structural Stability Theory

3.1. Establishment of calculation conditions

The objective of the calculation example presented here is to determine the required ground stiffness (i.e., deformation performance or rotational spring stiffness) necessary for the stability of a crawler crane. Additionally, the example seeks to examine the influence of load height on this required stiffness. The following outlines the conditions set for the calculations.

1) **Target equipment**

Hitachi Sumitomo Heavy Industries Construction Crane Co., Ltd. Crawler Crane, Model SCX400, 40 t×3.7 m [18].

2) **Calculation conditions**

Operating direction: 90 degrees (lateral direction is assumed for simplification).

The load is lifted statically (i.e., dynamic inertial forces are not considered). By setting an initial inclination angle θ_0 and statically lifting the load, the toppling stability criterion diagram (load–deformation angle relationship) shown in Figure 8 can be applied.

(The counterweight is 12.5 tonf; however, in this calculation example, it is considered only as part of the total weight and has no separate influence.)

Rotation center and boom base:

The rotation center and the base of the boom are both assumed to be located at the midpoint between the crawler centers, that is, S/2 = 3.3 m/2 = 1.65 m. In order to apply the structural model shown in Figure 2, the rotation center (support point) and the boom base are treated as coincident. Although in practice these

may differ, this simplification is adopted in light of the study's objective—to evaluate the influence of load height under structural stability theory.

Operating radius, boom length, and suspended load:

The analysis is conducted by categorizing the conditions into the following five groups. For further details, refer to Figure 6 and Tables 2 and 3.

Condition [1]: Operating radius a = 0 (initial inclination angle $\theta_0 = 0$), suspended load P_u = 10 tonf

For the upright condition, the boom length (load height) is varied to determine the critical load and the required ground stiffness using Equation (1). In this case, the overturning moment is zero.

Condition [2]: Operating radius a = 10 m, suspended load P_u = 10 tonf

For a condition with an initial inclination angle, the boom length is varied to determine the critical load and the required ground stiffness. Here, the overturning moment remains constant.

Condition [3]: Operating radius a = 10 m, suspended load $P_u \approx 5$ tonf

In this case, the operating radius is doubled, and instead the load is halved compared to Condition [2], enabling a comparative analysis under altered conditions.

Condition [4]: Operating radius a = 10 m, boom length L_B = 40 m

With a fixed operating radius and boom length, the suspended load is varied to determine the required ground stiffness.

Condition [5]: Initial inclination angle of 5 deg., boom length L_B = 40 m

This condition assumes a working inclination angle of 5 deg., as typically observed during pile driving operations [20], with variation in the magnitude of the suspended load.

Within each of the above condition groups, three to four specific cases are defined. These are indicated in the working range diagram (boom length–operating radius diagram) shown in Figure 6. The calculation results are presented in Table 2 for Conditions [1] through [4] and in Table 3 for Condition [5].

3.2. Procedures for stability calculation

In this section, based on the structural stability theory discussed thus far, the procedures for toppling stability evaluation and a specific example of its application are presented. The objective is to determine the required ground stiffness—either the rotational spring stiffness K_S (tonf·m/rad.) or the ground subgrade reaction coefficient k_v (tonf/cm)—necessary to prevent toppling under given conditions, such as load, boom length, and operating radius. These values represent the critical (neutral) limits at which toppling occurs. By comparing these computed neutral values with the actual properties of the ground, the safety margin can be evaluated.

The procedure and example calculation are outlined in the bullet points (①–⑩) below. The geometric relationships relevant to these calculations are illustrated in Figure 11. The example provided corresponds to the evaluation Case [2] (1) (or alternatively [4] (10)), with a summary of the results listed in Table 2 [1–4]. Figure 11

① Set the evaluation conditions:

Condition [2] (1): Suspended load P = 10 tonf, operating radius a = 10 m, boom length L_B = 40 m.

(The initial inclination angle θ_0 = 12.3, as obtained from the software "Crane Ground Pressure Simulation" on the website of Hitachi Sumitomo Heavy Industries Construction Crane Co., Ltd. [21]).

Figure 11
Stability limit angle

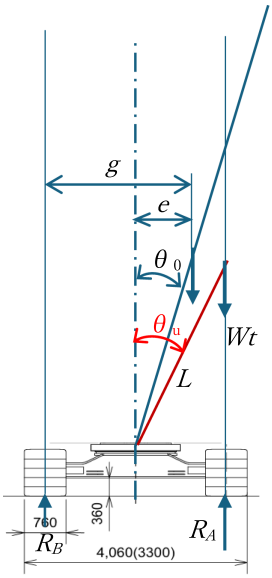

② Determine the toppling load (total weight) P_u (=W_t) = 54.2 tonf, and the reaction forces R_A = 47.8 tonf and R_B = 6.4 tonf: These values are also obtained by the aforementioned "Crane Ground Pressure Simulation [21]".

③ Calculate the horizontal distance "g" from the center of gravity to the midpoint between tracks (based on the reaction force R_B), and the horizontal distance "e" from the support point to the center of gravity (see Figure 11): $g = S \cdot R_A/W_t = (3.3)(47.8)/54.2 = 2.910$ m, $e = g – S/2 = 2.910 – 3.3/2 = 1.260$ m.

④ Calculate the boom length L from the rotation center to the center of gravity based on the horizontal distance e and the initial inclination angle θ_0 (see Figure 11). This length L is taken as the member length (load height) in the structural model (Figure 1): $L = e / \sin\theta_0 = 1.260/\sin 0.215 = 5.916$ m.

⑤ Using the member length L and the rotation center (half the crawler gauge), calculate the critical toppling angle θ_u and the ratio θ_0/θ_u (see Figures 12 and 3(b)): $\theta_u = \sin^{-1}(1.65/5.916) = 0.283$ rad., $\theta_0/\theta_u = 0.215/0.283 = 0.760$.

⑥ Calculate the critical load P_{cr} from $P_u/P_{cr} = 1 – \theta_0/\theta_u$ (Equation (3)):

$P_u/P_{cr} = 1 – 0.760 = 0.240$, $P_{cr} = 10/0.240 = 41.6$ tonf.

⑦ Calculate the required rotational spring stiffness (refer to Equation (1)):

$K_S = P_{cr} \cdot L_B = 41.6 \times 40 = 1663$ tonf·m/rad.

⑧ Calculate the force applied to the crawler per one radian of rotation based on the rotational spring stiffness: $R_{AB}^* = K_S/S = 1663/3.3 = 504$ tonf/rad.

(Note: See Figure 12 for the distribution of forces from the crawler to the ground.)

⑨ Calculate the required subgrade reaction coefficient k_v and ground settlement d:

$k_v = R_{AB}^*/165 = 504/165 = 3.05$ tonf/cm, $d = R_A/k_v = 47.8/3.05 = 15.6$ cm. These values k_v and d are directly related to the rotational spring stiffness K_S proportionally and inverse-proportionally, respectively.

(Note: See Figure 13 for the conversion factor 1 rad. = 165 cm.)

⑩ For reference, the P-θ curve (load–deformation curve) is shown in Figure 14, which is obtained by the equation $P = K_S (\theta – \theta_0)/(L_{cr} – \sin\theta)$ [14].

Figure 12
Coefficient of support strength k_v

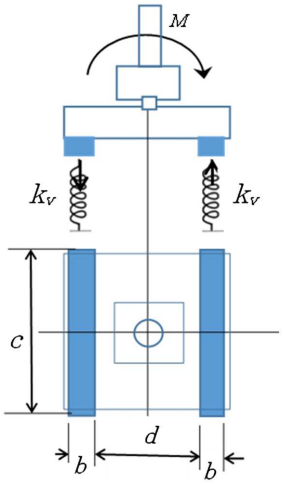

Figure 13
Factor of transformation

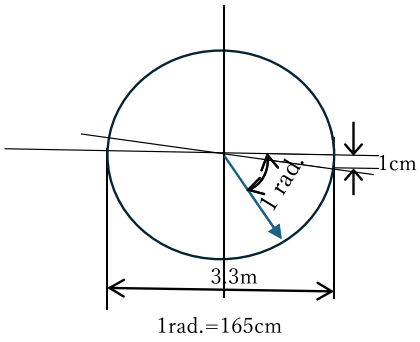

Figure 14
Load-displacement curve (1)(10)

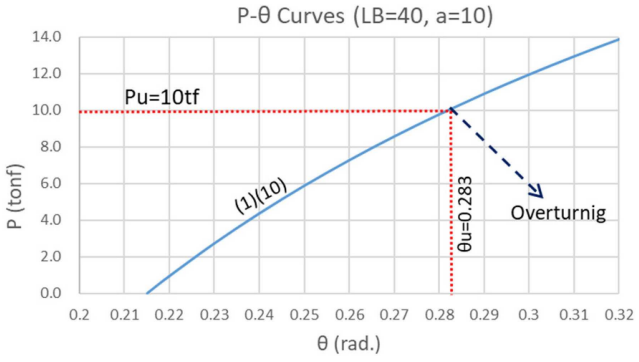

It should be noted that the computed values above correspond to a state in the process of toppling. In other words, when the load P_u = 10 tonf is reached, the deformation reaches the critical inclination angle (neutral value) θ_u = 0.283, as can be seen in Figure 14, and toppling due to ground failure is assumed to occur. In the structural stability diagram of Figure 15, this condition corresponds to point (1) on the diagonal line.

It is also important to note that the calculation assumes a static increase in load from zero to P_u, during which the boom angle θ/θ_u gradually increases. Therefore, the deformation angle ranges between θ_0 and θ_u. If, however, the boom angle is maintained at the initial inclination θ_0 by controlling the operation while slowly (statically) increasing the load, the inclination angle does not change—resulting in a safer operational method.

Figure 15
Results of stability safety status (static analysis)

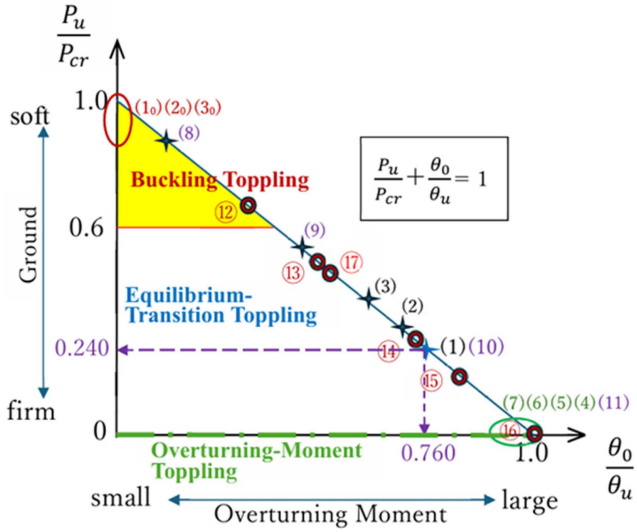

Remarks:

a) According to "Crane Ground Contact Pressure Simulation" [21], the maximum ground pressure is 3.32 kgf/cm^2 at the rear of the crawler with a slewing direction of 157 deg. Also, when the direction is 90 deg., it is shown as 1.61 kgf/cm^2 at the rear of the crawler.
b) The average ground pressure is calculated as total weight/crawler bottom surface area = 54,200 kgf/32,870 cm^2 = approximately 1.65 kgf/cm^2.

4. Results of Stability Calculations

4.1. Overview of structural stability characteristics

Tables 2 and 3 show the results for each calculation condition, following the procedures and calculation example described in the previous section. The first five rows from (a) to (e) are the calculation conditions (input parameters), and the rest are the calculated results as noted at the bottom of Table 2. Additionally, Figure 15 illustrates the structural stability characteristics, showing the position of each stability condition on the diagonal toppling line. In Figure 15, the structural stability diagram plots the load ratio of the first term in Equation (3) on the vertical axis and the overturning moment ratio of the second term on the horizontal axis. It should be noted that the calculation results represent the neutral values required for toppling under each condition.

From their positions, one can interpret the safety characteristics with respect to the vertical axis (ground stiffness safety, γ = actual ground reaction coefficient /required ground reaction coefficient) or the horizontal axis (overturning moment safety, $\nu = \theta_0/\theta_u$).

As previously mentioned, Table 2 classifies the calculation conditions for toppling into the following four groups:

Condition [1] Buckling-toppling type with an initial tilt angle θ = 0 (a = 0),

Condition [2] P_u = 10 tonf, and a = 10 m,

Condition [3] Toppling moment type with $P_u \approx 5$ tonf, and a = 20 m

Condition [4] Equilibrium transition type with L_B = 40 m, and a = 10 m.

For each of these conditions, the required rotational spring stiffness K_S (or required ground stiffness k_v) to prevent toppling is calculated. In the middle part of Table 2 [1–4], the maximum ground pressure *max p* (row (i)), the overturning moment M_t (row (j)), and the rated total load P_{rat} (row (k)) are shown for comparison with the structural stability-based evaluation method. Although these values are not directly comparable, they help illustrate the differences in the underlying concepts between the two approaches.

Table 3 presents the calculation results for Condition [5], which assumes a small initial tilt angle: L_B = 40 m, θ_0 = 5 deg. As seen in Figure 15, the toppling behavior for Condition [5] ranges broadly from buckling-toppling type to overturning moment type, similar to Condition [4]. In both conditions, the ground stiffness K_S ranges from very small to very large according to the magnitude of the load. However, it can be seen that the load range in the initial tilt angle θ_0 = 5 deg. (Condition [5]) is much larger than that of the initial tilt angle θ_0 = 12.3 deg. (Condition [4]). It should be noted that in all cases, the slewing direction of the boom is set at 90 deg.

4.2. Condition [1] with initial tilt angle $\theta_0 = 0$ (Cases: (1_0), (2_0), (3_0))

An initial tilt angle of zero indicates a condition where the boom is standing upright. According to the work range diagram in Figure 6, the positions for each case are directly above the support point. In this analysis, the boom length (i.e., the height of the suspended load) is varied across the three cases as follows: (1_0) L_B = 40 m, (2_0) L_B = 25 m, and (3_0) L_B = 16 m.

The goal is to examine how the required rotational spring stiffness K_S (or the required ground stiffness k_v) changes according to structural stability theory. Here, the suspended load is held constant at P_u = 10 tonf. For simplification, regardless of the procedure described in the previous chapter, the weight of other mechanical components is assumed to be concentrated at the support point. (In other calculation cases, the height of the load is determined based on the center of gravity of the total load, including both the suspended load and the machinery weight.) The total weight W_t varies slightly depending on the boom length, and since the tilt angle is zero, the reactions at the left and right crawlers R_A and R_B are equally divided.

For each calculation case, the load position of each condition is indicated on the work range diagram (Figure 6: boom length vs. working radius), and Figure 15 (stability characteristic diagram) shows that structural instability-type toppling occurs. In other words, because the initial tilt angle θ_0 is zero, all points lie on the apex of the vertical axis at P_u/P_{cr} = 1. This indicates that toppling occurs under conditions classified as pure "buckling-toppling type" according to structural stability theory [14].

Thus, buckling-toppling can occur even when cranes or pile drivers are in an upright position and is caused by extremely soft ground. Since the overturning moment is zero in this case, the current standard evaluation method—which is based on overturning moment—would conclude that toppling cannot occur. However, in structural stability theory, if the load exceeds the critical limit expressed by Equation (1), instability and toppling will occur. This critical limit has been verified through both numerical analysis and experimental results, similar to the buckling load of long columns [14, 15].

Comparing cases (1_0), (2_0), and (3_0) in Table 2 [1], the current evaluation method shows little difference in the maximum ground pressure (row (s), *max p*). However, according to structural stability theory, the required rotational spring stiffness K_S (or ground reaction coefficient k_v) increases as the boom length (i.e., load height) increases. This indicates that the higher the load, the lower the stability, and thus greater rotational spring stiffness (or greater ground stiffness) is required to prevent toppling. This highlights the significant impact of load height in toppling problems on soft ground, that is, an effect that is equally relevant to all other types of toppling issues.

4.3. Condition [2] with P = 10 tonf and a = 10 m (Cases: (1), (2), (3))

This section aims to compare with Condition [1] in Table 2, using a constant load of P = 10 tonf and the same boom lengths: (1) 40 m, (2) 25 m, and (3) 16 m, while varying the working radius to a = 10 m. Figure 6 (boom length vs. working radius diagram) shows the load position of each condition [18].

Figure 16 illustrates a comparison of the required ground reaction coefficient k_v between Conditions [2] and [1]. In Condition [1], since the initial tilt angle is zero, only the first term of Equation (3) applies, resulting in a very small required ground stiffness k_v. In contrast, under calculation Condition [2], an overturning moment is present, so the second term of Equation (3) also contributes, thus increasing the required ground stiffness accordingly. This difference is illustrated in Figure 16.

However, it should be noticed that the gravity center of the crane in Condition [1] is assumed to be located at the supporting point as mentioned previously, which differs from other conditions. This may cause an irrationality that the k_v of [2] is smaller than that of [1].

In calculation Condition [2], the three cases, that is, (1), (2), and (3), have the same load P_u = 10 tonf and working radius a = 10 m. Therefore, excluding the differences due to boom weight, there is no difference in the overturning moment (M_t) or the maximum ground pressure (*max p*). (Note that, when determining the maximum ground pressure, the boom's slewing direction is chosen so that the pressure is maximized.)

According to the current standard, stability is evaluated based on whether the ground can withstand this maximum ground pressure. As a result, there is little variation between the cases under this condition, and the rated total load P_{rat} is also close with each other, that is, between 9.15 and 9.7 tonf, as shown in blue in Table 1. (On the other hand, the assumed load in this Condition [2] is constant P_u = 10 tonf, which is slightly higher.) However, as shown in Figure 16, the required ground reaction coefficient k_v differs by approximately 3.5 times between cases (1) and (3). These differences will be revisited and further discussed in Section 4.7.

Figure 16
L_B - k_v curves

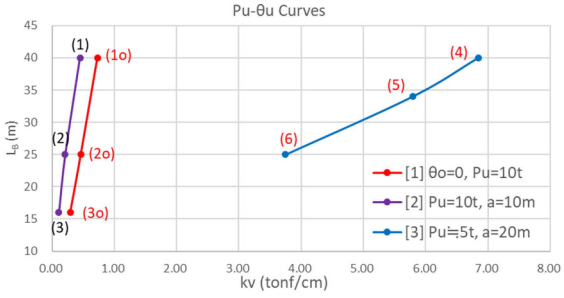

In addition, the structural stability diagram in Figure 15 shows the positions (marked along slanted lines) corresponding to the toppling state of each case. Although there are slight differences between cases (1), (2), and (3), all fall into the "*equilibrium transition type*" of toppling [14]. For case (1), it can be observed that the load ratio of the first term is 0.240, while the inclination term (second term) is relatively large at 0.760, which expresses the contribution ratios, respectively.

4.4. Condition [3] with $P \approx 5$ tonf and $a = 20$ m (Cases: (4), (5), (6), (7))

Next, in comparison with Condition [2], we examine the case where the working radius is doubled to $a = 20$ m, while the load is approximately halved to around 5 tonf. As shown in Figure 6 (boom length–working radius diagram), the load positions of these calculation conditions indicate that the working radius is larger than in Condition [2], which results in a larger initial tilt angle θ_0.

In Condition [3], the load P_u of approximately 5 tonf exceeds the rated total load of about 3.5 tonf. (Remarks: Table 1 shows that the rated load P_{rat} is defined to be within 78% of the toppling load, which means the toppling load is 3.5/0.78 = 4.5 tonf [18]. In other words, the overturning moment M_t might exceed the resisting moment M_r).

On the other hand, the structural stability diagram (Figure 15) indicates that, compared to the previous Condition [2], these cases are located near $\theta_0/\theta_u \approx 1.0$, and thus represent the *"overturning moment type"* of instability (refer to row (p)). This means the initial tilt angle θ_0 is large and nearly equal to the stability limit angle θ_u, indicating that there is almost no margin before toppling occurs. Without high ground stiffness, even a slight increase in tilt would result in toppling.

As a result, the required ground stiffness K_S is an order of magnitude larger than in the previous Condition [2] (see row (s)). In particular, comparing cases (6) and (7), it can be seen that a slight difference in load (see row (a)) causes a large variation in the required ground stiffness (see row (s)). This is because, as the horizontal axis ratio θ_0/θ_u approaches 1.0, the critical load P_{cr} on the vertical axis approaches infinity, resulting in significant differences.

This type of toppling occurs on firm ground when the overturning moment exceeds the resisting moment and is categorized as the "*overturning moment type*" in conventional stability evaluation methods [14]. Therefore, the toppling of the overturning moment type is evaluated along the horizontal axis in the structural stability diagram (Figure 15) based on structural stability theory. When the overturning moment M_t approaches the resisting moment M_r, very high ground stiffness is required. However, since actual ground conditions are rarely perfectly firm, even a slight insufficiency in stiffness could potentially lead to toppling.

4.5. Condition [4] with $L_B = 40$ m and $a = 10$ m (Cases: (8), (9), (10), (11))

Here, to compare with Condition [2] (1), which is considered likely to result in an *equilibrium transition type* of toppling, the boom length is fixed at $L_B = 40$ m and the working radius at $a = 10$ m (initial tilt angle $\theta_0 = 12.3$ deg.). The load P_u is varied as 5, 7.5, 10, and 12.5 tonf. If these conditions are plotted in Figure 6 (boom length–working radius diagram), they all correspond to the same point as Condition [2](1). Accordingly, as shown in Table 1, the rated total load P_{rat} for all these cases is the same 9.15 tonf [18]. However, it should be noted that the calculation results in Table 2[4], which indicate the required ground stiffness (row (s)) at the point of toppling for each different load, differ significantly.

Figure 17
P_u -θ_u curve

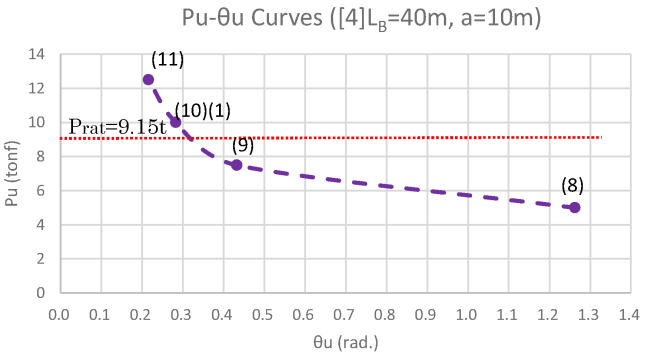

Figure 17 shows the relationship between the toppling load P_u and the corresponding toppling tilt angle θ_u. In the case of a smaller load, such as Case (8), the toppling tilt angle θ_u is large, meaning there is a sufficient margin before toppling occurs (the second term θ_0/θ_u of Equation (3) is small). As the load increases, θ_u becomes smaller; the contribution of the second term of Equation (3) θ_0/θ_u becomes larger as can be seen in Table 2 row (p).

Especially, for this crane model (SCX400), near the rated total load P_{rat} 9.15 tonf, even a slight change in the stability angle θ_u can significantly affect stability. In other words, in the vicinity of the rated load P_{rat}, a small variation in θ_u results in a large change in the toppling load.

A similar trend can be observed in Figure 18, which shows the relationship between the toppling load P_u and the required ground reaction coefficient k_v. In the vicinity of Case (10), where the toppling load $P_u = 10$ tonf slightly exceeds the rated total load $P_{rat} = 9.15$ tonf, the required ground stiffness increases rapidly. In Case (11), where the toppling load $P_u = 12.5$ tonf significantly exceeds the rated load, the required ground stiffness becomes nearly infinite. Incidentally, since the rated load is defined as 78% of the toppling load, the corresponding toppling load is $P_u = 9.15/0.78 = 11.7$ tonf [18].

4.6. Condition [5] with $L_B = 40$ m and $\theta_0 = 5$ deg.

Here, Condition [5] is considered in which the crane has a long boom length of 40 m and a small initial tilt angle of 5 deg., similar

Figure 18
P_u -k_v curve

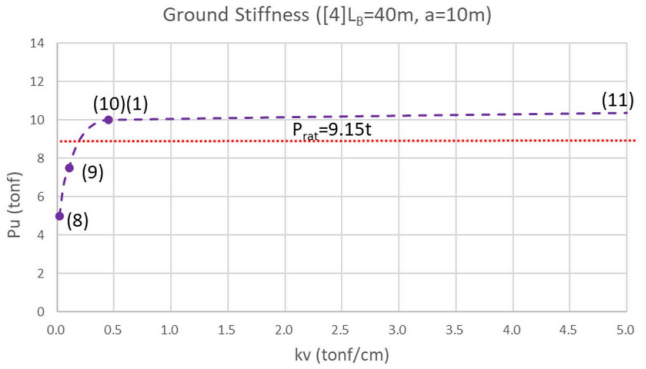

Figure 19
***P_u -θ_u* curve**

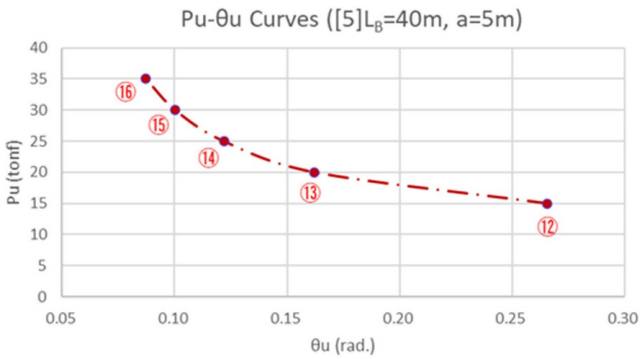

Figure 20
***P_u -k_v* curve**

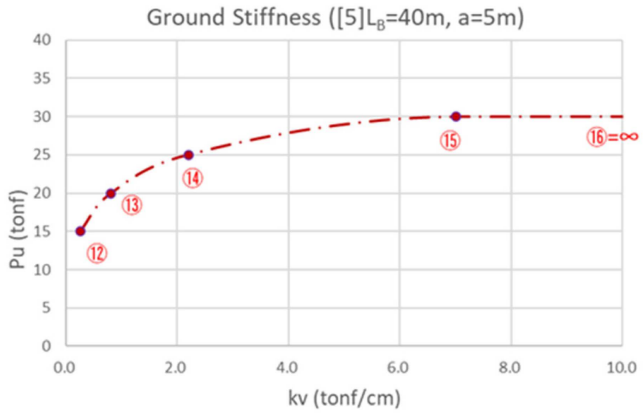

Figure 21
***M_t -k_v* curves**

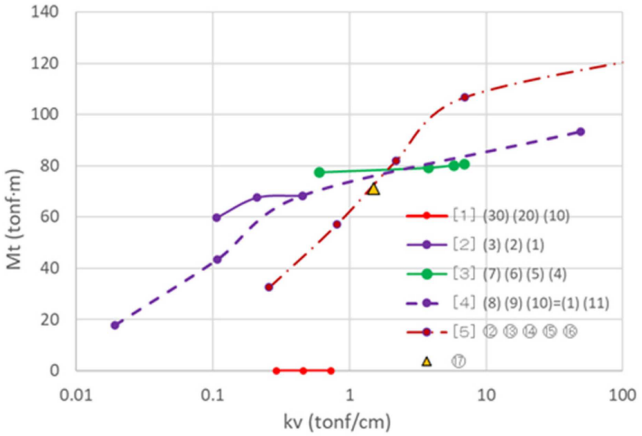

Figure 22
***M_t -max p* curves**

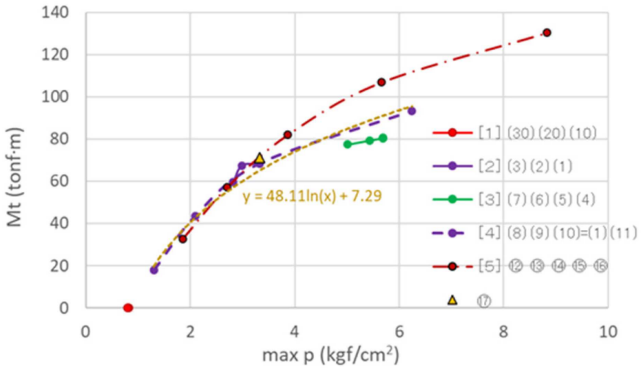

to that of a pile driver. The calculation results for this condition are shown in Table 3. However, because the initial tilt angle is smaller than in the previous conditions, the resulting toppling load becomes extremely large, and thus the rated load of the crane is not listed in Table 1 (as it falls outside the applicable range) [18].

The relationships between the toppling load P_u and the toppling tilt angle θ_u, as well as between the toppling load P_u and the required ground reaction coefficient k_v, are shown in Figures 19 and 20, respectively. According to the stability diagram in Figure 15, the toppling behavior of Condition [5] spans a wide range—from buckling-toppling type (Case ⑫) to overturning moment type (Case ⑯), similar to the distribution seen in Condition [4].

Thus, the behaviors of Condition [5] shown in Figures 19 and 20 are very similar to those in Figures 17 and 18 for Condition [4], in terms of the relationship between toppling load, tilt angle, and ground reaction coefficient. These figures reveal that the rate of change in required tilt angle or ground stiffness varies depending on the load range. In ranges with high rates of change, small prediction errors are more likely to result in accidents.

As seen by comparing the static analysis diagram of Figure 15 with the dynamic analysis diagram of Figure 10, the equilibrium transition type of Cases ⑫–⑮ falls into a range where dynamic analysis indicates significantly stricter toppling conditions. One of the factors making toppling more likely during movement or slewing, when dynamic inertial forces are generated, may be this characteristic.

4.7. Consideration from the overturning moment

This section compares the current stability evaluation method and the structural stability theory based on the magnitude of the overturning moment M_t (see row (j) in Table 2 [1–4]). Figure 21 shows the curve of overturning moment versus ground reaction coefficient (M_t- k_v) based on structural stability theory, while Figure 22 shows the curve of overturning moment versus maximum ground pressure (M_t -*max p*) based on the current stability evaluation method. In Figure 22, if the overloaded part of Condition [5] is excluded from the approximation curve, then the approximation aligns well with the calculation results. This is rational since the maximum ground pressure is derived directly from the overturning moment.

On the other hand, in Figure 21, it should be noticed that the horizontal axis k_v (ground reaction coefficient) is on a logarithmic scale; therefore, even for the same overturning moment, the required ground stiffness varies significantly. For example, in Figure 21, Condition [4] ranges from Case (8)—a buckling-toppling type, to Case (11)—an overturning moment type, showing a wide variety of toppling behaviors (refer to Figure 15). While in Figure 22 the difference between the maximum and minimum values of *max p* is within several times, in Figure 21 the difference in required ground stiffness k_v spans several tens of times.

Similarly, in the transition from Case (4) to (7) under Condition [3], the overturning moment is roughly the same; therefore, the maximum ground contact pressure *max p* does not differ much (see

Figure 23
Toppling scenarios

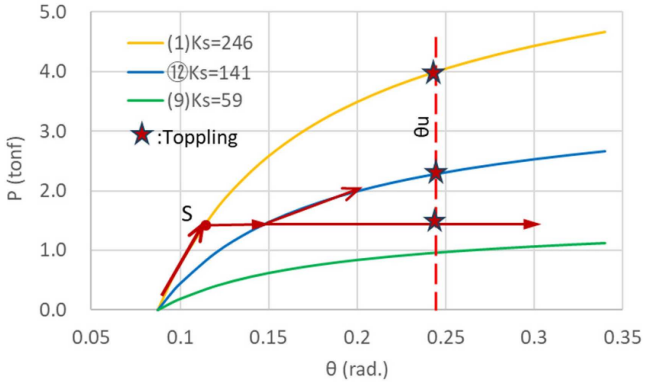

Figure 22); however, the required ground stiffness k_v differs significantly (see Figure 21). In other words, the variation in necessary ground stiffness to prevent toppling is much larger than the variation in the required maximum ground pressure. This same phenomenon can be observed in other cases as well.

Based on the above considerations, it is dangerous to judge toppling stability solely from the overturning moment or ground contact pressure (bearing capacity of the ground). It is believed necessary to also take into account the influence of ground stiffness (deformation performance) based on structural stability theory. The height of the load has a significant influence in this context. In reality, unexpected factors can easily arise with ground stiffness, and even a small trigger could lead to toppling.

5. Toppling scenarios

Toppling accidents involving cranes and similar heavy machinery are considered to occur due to factors outside the operator's expectations. Based on the findings from structural stability theory, the scenarios of unexpected toppling are discussed in the following two categories:

1) **Toppling due to load increase**

Load increase can occur during hoisting or as a result of centrifugal force during slewing operations. If the operation is conducted slowly enough, the load can be treated as static. However, if the rate of change is fast, the inertial force due to dynamic effects must be considered as explained above in Figure 9 [14]. Such predictions are believed to be difficult to make at actual work sites: note that the dynamic effects are not considered in the numerical investigation in Tables 2 and 3.

2) **Toppling due to weak ground**

Unexpected ground weakness is often encountered while moving or during an increase in hoisted load. The situation when moving from sufficiently firm ground to weak ground is illustrated by the load–deformation curves in Figure 23. Suppose that during movement, a load of approximately 12 tonf (point S) is applied under Condition (1) with sufficient ground strength, K_s = 246 tonf·m, and unexpectedly encounters a weaker ground with Condition ⑫, K_s = 141 tonf·m. At that moment, the load–deformation curve shifts to curve ⑫ in Figure 23, eventually reaching the critical toppling inclination angle θ_u. Furthermore, if the ground condition shifts to an even softer one, such as Condition (9), K_s = 59 tonf·m, the toppling inclination angle is reached even more rapidly. In this case, considering the dynamic inertial force caused by the sudden change, the likelihood of toppling is expected to increase even further.

6. Conclusions

This paper supplements conventional stability assessment methods based on the idea that preventing repeated crane and pile driver toppling accidents requires a structural stability perspective. The traditional approaches—comparing overturning moments with resisting moments, or applied ground pressure with soil bearing capacity—appear insufficient to fully ensure safety against toppling. Structural stability theory points out that toppling can occur not only due to insufficient ground strength under maximum ground pressure but also due to inadequate deformation performance. This paper demonstrates the impact of such factors through specific calculation examples.

Structural instability refers to toppling that can occur even when the overturning moment is zero, and in such cases, the height of the applied load, which has not traditionally been emphasized in toppling problems, plays a critical role. Through a range of detailed examples, this paper illustrates how load height is closely related to stability. The findings are summarized as follows.

1) Toppling accidents are more likely to occur when the center of gravity is high.
2) The working range diagrams (ground height vs. working radius) and rated load charts used in the current stability evaluation of cranes and pile drivers reflect safety against toppling due to overturning moments, but they do not take into account the effect of the center of gravity (i.e., load height).
3) According to stability evaluation based on structural stability theory, as the height of the center of gravity increases, toppling stability decreases, and greater ground stiffness (i.e., deformation performance) is required to maintain stability.

In this study, there are many simplifications in the structural model and analytical procedures. The boom rotation direction was fixed at 90 deg. to simplify the explanation of the structural stability-based toppling mechanism. However, future investigations should evaluate the rotational spring stiffness K_S for all directions, including oblique orientations. Additionally, this study employed a simplified structural model consisting of a rigid bar and rotational spring system, and certain assumptions were made—such as estimating the center of gravity from publicly available data and treating the boom base and support point as identical—which may differ from actual conditions. Nonetheless, the purpose of this paper is to clarify the influence of load height from the perspective of structural stability theory, which is not addressed in conventional stability evaluation methods. As such, the simplifications adopted here are considered acceptable within the scope of the study.

Moving forward, it will be necessary to conduct an experimental study to verify by comparing with the numerical results in this paper. Also, analyses are expected based on more precise data and to deepen the understanding of the relationship between rotational spring stiffness and supporting ground characteristics in collaboration with geotechnical engineering. Furthermore, incorporating dynamic analysis into the assessment of toppling stability will be essential. It is hoped that a more detailed understanding of the toppling mechanism based on structural stability theory will contribute to a reduction in toppling accidents.

Acknowledgment

The authors would like to express our sincere appreciation to Sumitomo Heavy Industries Construction Crane Co., Ltd. for making available the data on the crawler crane SCX400 through their

website's "Crane Ground Pressure Simulation." This information was very helpful in carrying out this study.

Ethical Statement

This study does not contain any studies with human or animal subjects performed by any of the authors.

Conflicts of Interest

The authors declare that they have no conflicts of interest to this work.

Data Availability Statement

Data are available on request from the corresponding author upon reasonable request.

Author Contribution Statement

Shouji Toma: Conceptualization, Methodology, Formal analysis, Investigation, Data curation, Writing – original draft, Writing – review & editing, Visualization. **Wai Fah Chen:** Validation, Supervision, Project administration.

References

[1] Toma, S., & Chen, W. F. (2024). A study on safety criteria for toppling of pile drivers and Cranes based on structural stability. *Archives of Advanced Engineering Science*, *3*(2), 93–99. https://doi.org/10.47852/bonviewAAES42022138

[2] JCMA. (2023). Crane related accidents-examples of disaster, *Japan Construction Machinery and Construction Association*. Retrieved from: https://jcmanet.or.jp/saigai-jirei/ (in Japanese)

[3] FAJFCG. (2023). Accidents 100, collection of examples, *Federation of All Japan Foundation Construction Group, General Inc., Association*. Retrieved from: http://www.kt.rim.or.jp/~zenkiren/contents/jiko100.html, (in Japanese)

[4] Skiba, R. (2024). *Crane operations*.UK: After Midnight Publishing.

[5] Doci, I., Lajqi, N., & Lajqi, S. (2018). Crawler Crane overturning analysis for the case of boom luffing motion. *International Review of Mechanical Engineering*, *12*(2), 135. https://doi.org/10.15866/ireme.v12i2.14358

[6] Zhou, Q., Liu, Y., Xie, Y., & Zhang, X. (2022). Analysis on anti-overturning stability of a truck Crane based on zero moment point theory. *Dyna (Bilbao)*, *97*(3), 281–287. https://doi.org/10.6036/10484

[7] Jang, H., Lee, Y., Lee, H., & Park, J. (2024). Preventing overturning of mobile cranes using an electrical resistivity measurement system. *Applied Sciences*, *14*(21), 9623. https://doi.org/10.3390/app14219623

[8] Queensland Code of Practice. (2024). Mobile Crane, workplace health and safety. Queensland, Australia, Mobile crane Code of Practice 2024.

[9] Hambly, E. C. (1990). Overturning instability. *Journal of Geotechnical Engineering*, *116*(4). https://doi.org/10.1061/(ASCE)0733-9410(1990)116:4(704)

[10] Eskişar, T., & Akboğa Kale, Ö. (2022). Evaluation of pile driving accidents in geotechnical engineering. In*ternational Journal of Occupational Safety and Ergonomics*, *28*(1), 625–634. https://doi.org/10.1080/10803548.2019.1685195

[11] Fukagawa, R., Muro, T., Kato, Y., & Morita, Y. (1994). An analysis of overturning conditions of truck Crane considering possible ground failure. *Doboku Gakkai Ronbunshu*, *1994*(504), 61–70. https://doi.org/20.2208/jscej.1994.504.61

[12] Tamate, S., & Hori, T. (2010). Safety requirements for prevention of overturning by drill rigs and piling equipment in consideration of the potential of instability. *JNIOSH-SDNO28, Safety Documents of the National Institute of Occupational Safety and Health*, *NIOSH-SD-NO.28 (2010) UDC 624.131.524: 624.131.526: 624.131.37: 621.868.27: 614.822: 624.046 (in Japanese)*.

[13] Tamate, S., & Hori, T. (2015). A study on safety practices of investigation of bearing capacity of supporting ground for prevention of overturning of heavy machineries. *Technical documents of the National Institute of Occupational Safety and Health*, *NIOSH-TD-NO.3 (2015) UDC 624.155.15: 621.873.3: 625.032.7: 624.131.383: 624.131.524: 539.4.012: 624.159.2 (in Japanese)*.

[14] Toma, S., Seto, K., & Chen, W. F. (2024). Comparisons of static and dynamic analyses on toppling behaviors of pile driving machinery, etc., on soft foundation. *Archives of Advanced Engineering Science*, *2*(3), 150–159. https://doi.org/10.47852/bonviewAAES32021602

[15] Toma, S., & Chen, W. F. (2024). Capsizing mechanism of self-elevating platform based on structural stability theory. *Current Trends Civil & Structural Engineering*, *11*(3), CTCSE.MS.ID.000765. https://doi.org/10.33552/CTCSE.2024.11.000765

[16] ICOPCA. (2014). Interim summary of the investigation and consideration of the Okinotorishima port construction accident, investigative committee for the Okinotorishima port construction accident, Kanto Regional Development Bureau, Port and Airport Department. *Ministry of Land*. Infrastructure, Transport and Tourism (in Japanese).

[17] Doya, Y., & Sawada, T. (2021). Stability index as a floating body of rectangular hull. *Journal of the Japan Society of Naval Architects and Ocean Engineers*, *33,* (63–72) (in Japanese).

[18] HSC. *SCX400 Hydraulic Crawler Crane Specifications*. *Hitachi Sumitomo Heavy Machinery and Construction Crane, Co. Ltd*. Retrieved from: https://www.hsc-cranes.com/data_files/scx400_sp_jp.pdf.NIPPON

[19] JCMA. (2013). Manual of Maintaining Support Foundation for Mobile Crane, Pile Drive, etc., Ver. 2. *Japan Construction Machinery and Construction Association* (in Japanese).

[20] SHARYO, LTD. (2014). Basic guideline for safety operation, document no. H3-BH-2750D, revised on December 15, 2014, safe_guideline.pdf (n-sharyo.co.jp) (in Japanese).

[21] HSC. *Simulation for Ground Pressure of Crane. Service & Support, Hitachi Sumitomo Heavy Machinery and Construction Crane, Co. Ltd*. Retrieved from: https://www.hsc-cranes.com/jp/support/simulation, (in Japanese).

How to Cite: Toma, S., & Chen, W. F. (2025). Numerical Study on Toppling Mechanisms of Crane and Pile Driver Based on Structural Stability Theory. *Archives of Advanced Engineering Science*. https://doi.org/10.47852/bonviewAAES52026150